Received 12 September 2023; accepted 26 September 2023. Date of publication 2 October 2023; date of current version 17 October 2023.

Digital Object Identifier 10.1109/OJCOMS.2023.3321136

Unified Constellation Design Using Projection Over QAM: Concept and Examples

XIAORUI YAN[1], PEISEN WANG[1], AIHUA WANG[1] (Member, IEEE), WENJIA LIU[2], XIAOLIN HOU[2] (Senior Member, IEEE), JUAN LIU[2], AND NENG YE[3] (Member, IEEE)

[1]School of Information and Electronics, Beijing Institute of Technology, Beijing 100081, China
[2]Wireless Technology Department, DOCOMO Beijing Communications Laboratories Company Ltd., Beijing 100081, China
[3]School of Cyberspace Science and Technology, Beijing Institute of Technology, Beijing 100081, China

CORRESPONDING AUTHORS: N. YE AND P. WANG (e-mail: ianye@bit.edu.cn; wps@bit.edu.cn)

This work was supported in part by the National Natural Science Foundation of China under Grant 62101048, Grant 62171030, and Grant 62071038; in part by the National Key Research and Development Program of China under Grant 2022YFC3301404; in part by the China Postdoctoral Science Foundation under Grant 2022M710394 and Grant 2022T150053; and in part by the Young Elite Scientists Sponsorship Program by CAST under Grant 2022QNRC001.

ABSTRACT Beyond fifth generation (B5G) / sixth generation (6G) wireless systems require full utilization of all spectrums. However, hardware devices operating in the high-frequency bands bring a series of non-ideal behaviors, including nonlinear distortion caused by high-power amplifiers and phase noise generated by radio-frequency oscillators, which will lead to performance degradation of traditional signal modulation technology. To this end, this paper proposes a 5G new radio-compatible constellation design method using projection over quadrature amplitude modulation (QAM). First, to address the nonlinear distortion caused by power amplifiers, the pseudo-amplitude-phase-shift keying (APSK) constellation with a low peak-to-average power ratio is proposed. The signal points are selected from QAM by minimum Euclidean distance with APSK. Second, for a phase noise channel, the pseudo-spiral constellation is designed with the projection of Spiral constellation points onto QAM by the proposed minimum radial-angular weighted distance. Simulation results show that the proposed pseudo-APSK modulation outperforms traditional QAM at medium and high code rates considering nonlinear distortion produced by a power amplifier. Besides, the proposed pseudo-spiral modulation exhibits significant performance gain and improved robustness compared to QAM under phase noise-affected channels, particularly in medium-high signal-to-noise ratio conditions.

INDEX TERMS APSK, B5G/6G, constellation design, phase noise, power amplifier, QAM, spiral.

I. INTRODUCTION

IN THE future, high-rate wireless communication is expected to support wider spectral bandwidth and make full use of various carrier frequencies. Thus, higher frequencies such as mmWave and Terahertz (THz) are considered to meet the requirements of beyond fifth generation (B5G) and sixth generation (6G) networks [1], [2]. However, for high-frequency broad bandwidth systems, hardware impairments can lead to severe nonlinear signal distortions and performance degradation of traditional signal modulation technologies [3], [4]. On the one hand, the nonlinearity of the power amplifier (PA) causes amplitude distortion and phase shift of the modulated signal. On the other hand, phase noise (PN) generated by high-frequency oscillators causes the modulated signal to encounter dispersion at the angle and suffer from strong phase impairments. At present, quadrature amplitude modulation (QAM) has been adopted in fifth generation (5G) new radio (NR) of 3rd Generation Partnership Project (3GPP) standards [5], but it is unsuitable to be directly transposed to B5G/6G for its poor performance under non-ideal conditions of hardware devices. In addition, the construction of the integrated space and terrestrial network (ISTN) has become a significant trend of 5G and 6G communication networks to realize global coverage (land, air, space, sea) [1], [6], [7], which makes compatibility with existing systems meaningful. Consequently, a unified constellation design will be needed to support both terrestrial and non-terrestrial networks (NTN), as well as to

mitigate the effects of hardware impairments. It is necessary to re-evaluate modulation technologies and design constellation diagrams available for high-frequency, high-data rate transmission with backward compatibility.

A. LITERATURE AND MOTIVATION

Efforts have been made to improve the performance of communication systems impaired by PA nonlinearity and PN. For example, one approach to resist PA nonlinearity is to reduce the peak-to-average power ratio (PAPR) of transmitted signals based on encoding methods, constellation modulation or waveform design. For a PN channel, improvements can be made from both the receiver and transmitter sides. In particular, this section mainly introduces literature on constellation optimization for PAPR reduction and PN channels.

The constellation design for PAPR reduction before entering the power amplifier to reduce the non-linear distortion has been extensively studied. The carrier injection algorithm proposed in [8] modifies constellation points in multiple subcarriers to achieve PAPR suppression, increasing the size of the constellation so that each constellation point in the complex plane of the original constellation is mapped to several other points in the extended constellation before inverse discrete Fourier transform (IDFT) processing. Active constellation extension (ACE) is introduced in [9], [10], [11] to extend constellation points outward without reducing the minimum Euclidean distance between constellation points, which can reduce PAPR while ensuring bit error rate (BER) performance. However, the signal transmission power becomes larger, which limits the applicability of high-order modulation schemes. Symmetric constellation extension (SCE) is proposed in [12], in which each constellation point is represented by two rotationally symmetric points. The basic idea is to use a deterministic and efficient algorithm to design optimum signs for each subcarrier of a multicarrier signal, modulated by any codeword, to reduce its peak to mean envelope power ratios (PMEPR). Reference [13] reduces PAPR for orthogonal frequency-division multiplexing (OFDM) systems in a probabilistic framework, aiming at the best representation of the data for each subcarrier. A de-randomization algorithm is used for an optimal representation of the OFDM signal either by points in the original constellation or by extended ones, which reduces the average transmission power by 0.64 dB compared with the SCE modulation scheme. The constellation shifting (CS) proposed in [14] breaks the traditional one-to-one bit-to-symbol mapping rule. The shifted 16QAM ensures a constant minimum Euclidean distance and obeys the rules of the Gray Code. A sequence of bits can be mapped to four candidate constellation points after shifting. The scheme saves power and allows the receiver to know the precise location of the shifted constellation points. The combination of two signal constellations is an effective solution to reduce PAPR as well [15]. Two constellation schemes are used to encode binary data in an OFDM symbol, and a suitable constellation is selected for each subcarrier to reduce PAPR. Its core idea is to apply an exhaustive search algorithm to find the best arrangement of two constellation schemes in an OFDM symbol, and then achieve PAPR suppression.

In addition to the above methods, constrained constellation formation is also an effective way to reduce PAPR by adjusting constellation points on the in-phase and quadrature (IQ) plane under certain constraints, such as average power normalization and maximum power normalization. The usual rules include maximizing the minimum Euclidean distance, maximizing mutual information (MI), and minimizing the BER. The representative one is amplitude-phase-shift keying (APSK) constellations C. Thomas et al. proposed. They first described the low PAPR characteristic of APSK in [16]. The Gray APSK proposed in [17] provides shaping gain for satellite communication, which proves that Gray APSK in bit interleaving coding systems has greater channel capacity and better block error rate (BLER) performance than QAM, and the gain is more obvious with the increase of modulation order.

Assuming a PN channel, it is found that phase noise will cause random rotation of the received signal, leading to phase impairments and detection errors. Besides, phase noise will destroy the orthogonality of subcarriers in OFDM systems, resulting in inter-carrier interference (ICI) and thus degrading system performance. The problem of compensating for systems affected by phase noise based on the optimization of the signal constellation to achieve coherent performance has been widely investigated in prior work. Several approaches have been considered, including the design method with the symbol error probability (SEP) or mutual information as the objective function, spiral constellation and circular constellation design, which are introduced respectively below.

Foschini et al. first started their research on the optimization of PN constellation in [18], which used a heuristic search to select signal points in the lattice to minimize the SEP with Tikhonov phase noise. In [19], constellations that are robust to phase noise with low decoding complexity were designed. In [20], the SEP of maximum likelihood (ML) detector with a given phase offset was derived, and a gradient descent algorithm was used to find the constellation minimizing the SEP. An iterative constellation optimization algorithm considering additive white Gaussian noise (AWGN) and phase noise was proposed in [21], which was applied to the square 16-QAM constellation. To mitigate the nonlinear phase noise in the coherent APSK system, two-stage (TS) ML detection, including amplitude detection and phase detection, was used in [22], [23], [24], and the low order APSK was optimized according to the TS detector to minimize the symbol error rate (SER). However, this kind of modulation scheme has poor performance under highly nonlinear conditions, and this suboptimal detection strategy requires accurate knowledge of the transmission link.

Under the assumption that both channel noise and phase noise are white noise, Kayhan and Montorsi proposed a fast

approximation method to compute the achievable mutual information (AMI) for a given constellation, and a simulated annealing algorithm was used to maximize the AMI under the average power constraint to obtain the optimal constellation in [25]. Based on [25], Krishnan et al. provided an analysis framework for constellation design by considering three optimization formulas to study constellation optimization under strong phase noise in [26]. It is proved that the optimized constellations are superior to traditional QAM, phase shift keying (PSK) and spiral QAM in SEP, error floor and MI. However, they do not have any specific structure, which can make their actual implementation complicated. In [27], Kayhan and Montorsi used the simulated annealing algorithm to optimize constellation and binary labels together. They considered pragmatic average mutual information (PAMI) as the objective function and further clarified the superiority of optimized constellations with 8, 16, 64 and 256 signals over conventional constellations.

Spiral constellation design is also a valid means to combat phase noise due to its geometric structure, which helps mitigate the impact of PN. In 2008, Kwak et al. proposed a method to design spiral QAM constellations [28]. The violent search algorithm is used to determine the bit-to-symbol mapping rules. Based on simulation results of BER performance, the validity of spiral QAM in the presence of phase noise is verified. However, the spiral design proposed here is based on a more computationally intensive process, and it does not allow constellations to be defined using closed-form expressions. Inspired by the geometric structure of the Archimedean spiral, Ugolini et al. placed constellation points on the Archimedean spiral and proposed spiral constellations based on the semi-analytic description in the Gaussian phase noise channel with an optimized spiral shape parameter f_s [29], [30]. Constellation points defined by an expression in a closed form allow for a simple design. Reference [30] compares the information rate (IR) and error rate performance of spiral constellations with QAM and APSK to prove the significant superiority of this modulation scheme.

Last but not least, it has been proved in [24], [31], [32], [33] that circular constellations whose points are on concentric circles may achieve performance gain over PN channels as well, including circular QAM, APSK, and the constellation defined upon a lattice in the amplitude-phase domain. For instance, the Polar-QAM scheme with efficient binary labeling and demodulation is proposed in [33], which provides performance gains and a low-complexity implementation.

To sum up, most of the existing solutions on constellation optimization for hardware impairments are not compatible with the modulation schemes in 5G NR. First, the IQ values of these optimized constellation points are not integers, which will increase the quantization error for digital processing. Besides, the bit-to-symbol mapping methods of these constellations are different from QAM, which may require different modulation or demodulation methods and transceiver structures. As a result, incompatible modulation schemes will be extremely inconvenient for future B5G/6G communication systems, such as the scenario of ISTN [34], [35], [36]. Thus, there is an urgent need for a unified constellation design method.

B. CONTRIBUTIONS

Different from previous work, in this paper, we propose an NR-compatible constellation design for high-frequency band transmission, considering the nonlinear distortion caused by a power amplifier and phase impairments due to phase noise. Based on a certain distance criterion, N-order constellation points are directly selected from M-QAM defined in 5G NR satisfying $M > N$ to approximate other constellation diagrams and gain additional benefits. Thus, N-APSK_M-QAM constellations with low PAPR and N-Spiral_M-QAM modulation with phase noise resistance are designed, respectively. By projecting signal points onto QAM, the new constellations obtained can be compatible with existing 5G modulation schemes. Meanwhile, they also retain the advantages of the original constellations before projection. The main contributions of this paper can be listed as follows:

1) We propose a B5G/6G-compatible unified constellation design using projection over QAM. This method provides a bridge and tool that matches state-of-the-art constellations optimized for hardware impairments with 5G standards to compensate for the performance deterioration of QAM under non-ideal conditions. Based on the concept of projecting constellation points over QAM, we then give two examples, including the design of pseudo-APSK and pseudo-spiral.
2) We propose an NR-compatible pseudo-APSK (pAPSK) constellation design to mitigate the nonlinear distortion caused by PA. N constellation points are selected from M-QAM by minimum Euclidean distance to form an N-APSK_M-QAM constellation. Meanwhile, Bit-to-symbol mapping rules are also designed, which multiplex the rules of APSK in digital video broadcasting (DVB) standard [37], [38]. Specifically, expressions in closed form are proposed for the bit-to-symbol mapping.
3) We propose an NR-compatible pseudo-spiral (pSpiral) constellation design to suppress the effect of phase noise. For the projection process under phase noise, a new distance criterion considering both the radial distance and the angular distance is designed. That is, the points are selected from QAM by using the proposed criterion of minimum radial-angular weighted distance. Moreover, we give the bit-to-symbol mapping method according to the spiral architecture and the rotation of points due to phase noise.
4) We evaluate the coded block error rate (BLER) performance of proposed pAPSK constellations, as well as the uncoded SER performance of pSpiral constellations. Simulation results show that the proposed N-APSK_M-QAM modulation scheme outperforms traditional N-QAM, especially under high code rates.

Besides, the proposed N-Spiral_M-QAM modulation is also superior to QAM and is more robust to phase noise change.

The rest of this paper is organized as follows: In Section II, the system models of PA response and PN channel are described. Besides, the design concept is also elaborated. Then, N-APSK_M-QAM and N-Spiral_M-QAM modulation schemes are introduced in Sections III and IV, respectively. Section V presents the simulation results of the proposed constellations. Finally, our work is summarized and concluded in Section VI.

II. SYSTEM MODEL AND DESIGN CONCEPT

In this section, we first give the modeling of the power amplifier response and the channel model affected by phase noise. Then, we explain the design concept of the proposed unified constellation design.

A. PA RESPONSE MODEL

The output power of an ideal power amplifier is linear to the input power, but it is difficult to achieve in practical power amplifiers. When the signal enters the non-linear region of a practical power amplifier, the output power tends towards its maximum value and no longer increases linearly with the increase in input power. Signals with PA working in the non-linear region will have amplitude and phase distortion, which are reflected in the constellation diagrams corresponding to the expansion and rotation of constellation points respectively. These two kinds of distortion are collectively called nonlinear distortion, which will seriously affect the reliability of the system. Besides, the intensity of nonlinear distortion will become stronger with the increase of signal amplitude. Herein, the input signal $x(t)$ and the output signal $y(t)$ after passing through the power amplifier are given by

$$\begin{aligned} x(t) &= A(t)\cos(2\pi f_c t + \theta(t)), \\ y(t) &= G[A(t)]\cos\big[2\pi f_c t + \theta(t) + \Psi(A(t))\big], \end{aligned} \tag{1}$$

respectively, where $G[A(t)]$ is the amplitude-to-amplitude modulation (AM-AM) distortion, a function describing the nonlinear distortion between the amplitude of the input signal $A(t)$ and the amplitude of the output signal with respect to the PA, and $\Psi(A(t))$ is the amplitude-to-phase modulation (AM-PM) distortion, representing the nonlinear distortion between the amplitude of the input signal $A(t)$ and the phase of the output signal for the PA.

Common models to characterize $G[A(t)]$ and $\Psi(A(t))$ include Saleh model, Rapp model, modified Rapp model and Ghorbani model [39]. Considering that the complementary metal oxide semiconductor (CMOS) is a commonly used power amplifier in practical communication systems, in this paper, we focus on the CMOS PA model and employ the modified Rapp model to characterize its amplitude and phase distortions within the high-frequency spectrum. According to [39], the AM-AM and AM-PM characteristics of the CMOS power amplifier are modeled as (2) and (3) respectively:

$$G(A) = g\frac{A}{\left[1+\left(\frac{gA}{A_{sat}}\right)^{2s}\right]^{\frac{1}{2s}}}, \tag{2}$$

$$\Psi(A) = \frac{\alpha A^{q_1}}{\left[1+\left(\frac{A}{\beta}\right)^{q_2}\right]}, \tag{3}$$

where A is the amplitude of the input signal, and the parameters used in the CMOS power amplifier model are as follows [39]: $g = 4.65$, $A_{sat} = 0.58$, $s = 0.81$, $\alpha = 2560$, $\beta = 0.114$, $q_1 = 2.4$, $q_2 = 2.3$.

B. PN SYSTEM MODEL

Assuming a complex AWGN channel with phase noise, the k-th received signal can be written as

$$y_k = x_k e^{j\phi_k} + n_k, \tag{4}$$

where x_k is the k-th transmitted constellation point, ϕ_k denotes the phase noise sample, and n_k is the complex Gaussian noise with variance σ_n^2, i.e., $n_k \sim \mathbb{C}\mathcal{N}(0, \sigma_n^2)$. The phase noise sample ϕ_k is assumed to have a zero-mean Gaussian distribution with variance σ_ϕ^2, i.e., $\phi_k \sim \mathcal{N}(0, \sigma_\phi^2)$.

The Gaussian noise samples n_k denote a set of independent identically distributed (i.i.d.) complex Gaussian random variables. The phase rotation ϕ_k represents the residual phase noise after the phase tracking and compensation of the received signal. Generally, the samples $\{\phi_k\}$ may be correlated. However, an ideal estimator which can remove any correlation is considered to simplify the analysis [18], [26], [40]. Thus, the residual PN impairments $[\phi_0, \ldots, \phi_{L-1}]$ stands for a memoryless phase noise process [41], where L is the number of received symbols. The transmitted symbol x_k is randomly picked up from the signal constellation $\{s_m, m \in \{1, \ldots, M\}\}$ of M points, and all the points are sent equally with the probability $1/M$. Note that x_k and ϕ_k are independent of each other.

C. DESIGN CONCEPT

This paper proposes a simple but effective 5G-compatible constellations design method for B5G/6G. In the proposed method, new constellations can be designed to meet different non-ideal factors faced by practical systems while ensuring backward compatibility with 5G NR. Specifically, N-order constellation points are projected onto QAM of M signal points based on a certain distance criterion, where M is generally greater than N.

Remark 1: The proposed method using projection over QAM provides a unified constellation design framework for practical wireless communication systems. It is a bridge and tool that can combine the constellations optimized for hardware impairments with 5G standards to compensate for the performance deterioration of QAM under non-ideal

conditions, with the aim of enhancing the flexibility and robustness of modulation schemes in practical communication systems in a straightforward and effective manner.

III. CONSTELLATION DESIGN OF QAM-COMPATIBLE PSEUDO-APSK

Based on the proposed design concept, in this section, we present an example of NR-compatible pseudo-APSK constellation design for nonlinear distortion caused by PA.

A. DESIGN PROCESS OF PSEUDO-APSK

Considering the low PAPR characteristic of the APSK constellation, which is beneficial for reducing the impact of PA nonlinearity, the DVB standard has taken APSK as the modulation scheme [37], [38]. In this section, N-order pAPSK constellation points are selected from M-order QAM to obtain low PAPR and compatibility with NR. The process of N-APSK_M-QAM constellation design is summarized as follows:

- First, an M-order QAM constellation is generated according to the modulation mapper specified in 3GPP TS 38.211 [5].
- Second, an N-APSK constellation is determined by the number of circles, the number of points on each circle, the radius and the initial phase of each circle. The parameters can be obtained from the DVB standard [37], [38] or through optimization.
- Third, we project N-APSK over M-QAM to get an N-APSK_M-QAM constellation. By using the method of exhaustive search, the constellation points of N-APSK and M-QAM are compared one by one. Then, N non-coincident points of M-QAM closest to the original N-APSK are selected based on the principle of minimum Euclidean distance to form N-APSK_M-QAM constellation.

With binary bits $\boldsymbol{b}$ as input and complex modulation symbols $\boldsymbol{s}$ as output, 16QAM, 64QAM and 256QAM modulation mappers are listed hereafter [5]:

In 16QAM modulation, every four bits $\boldsymbol{b}_k(0)$, $\boldsymbol{b}_k(1)$, $\boldsymbol{b}_k(2)$, $\boldsymbol{b}_k(3)$ are mapped into a complex modulation symbol s_k, where k represents the k-th modulated symbol. That is,

$$s_k = \frac{1}{\sqrt{10}}\{(1-2\boldsymbol{b}_k(0))[2-(1-2\boldsymbol{b}_k(2))] + j(1-2\boldsymbol{b}_k(1))[2-(1-2\boldsymbol{b}_k(3))]\}. \quad (5)$$

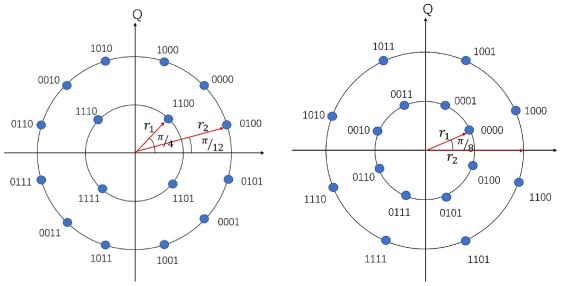

(a) (4+12)-APSK (b) (8+8)-APSK

FIGURE 1. (4+12)-APSK and (8+8)-APSK constellations.

In 64QAM modulation, every six bits $\boldsymbol{b}_k(0)$, $\boldsymbol{b}_k(1)$, $\boldsymbol{b}_k(2)$, $\boldsymbol{b}_k(3)$, $\boldsymbol{b}_k(4)$, $\boldsymbol{b}_k(5)$ are mapped into the k-th complex modulation symbol s_k, which can be expressed as (6), shown at the bottom of the page.

In 256QAM modulation, every eight bits $\boldsymbol{b}_k(0)$, $\boldsymbol{b}_k(1)$, $\boldsymbol{b}_k(2)$, $\boldsymbol{b}_k(3)$, $\boldsymbol{b}_k(4)$, $\boldsymbol{b}_k(5)$, $\boldsymbol{b}_k(6)$, $\boldsymbol{b}_k(7)$ are mapped into the k-th complex modulation symbol s_k, which can be expressed as (7), shown at the bottom of the page.

An APSK constellation is composed of R concentric circles, and points on each circle are equally spaced. APSK constellation set C can be given as

$$C = \left\{ r_k \cdot \exp\left(j\left(\frac{2\pi}{n_k} i + \theta_k \right) \right) \right\}; i = 0, 1, \ldots, n_k - 1, \quad (8)$$

where n_k, r_k, θ_k represents the number of constellation points on the k-th circle, the radius and the initial phase of the k-th ($k = 1, 2, \ldots, R$) circle, respectively. The APSK constellation can also be represented by $(n_1 + n_2 + \cdots + n_R)$ - APSK. In general, M constellation points will be subject to symbol energy normalization, i.e., $\sum_{k=1}^{R} n_k \cdot r_k^2 = M$. And the initial phase on each circle is set to $\theta_k = 0$ or $\theta_k = \frac{\pi}{n_k}$.

The first method to pick an N-APSK constellation is to select directly according to the parameter set and mapping rules given in DVB standard [37], [38]. For example, two different structures of 16APSK are given, including (4+12)-APSK and (8+8)-APSK, as shown in Fig. 1. Another method is to optimize an APSK constellation by maximizing minimum Euclidean distance or MI, which is equivalent to each other at high signal-to-noise ratio (SNR).

After the determination of N-APSK and M-QAM, we can use projection over QAM to obtain pAPSK. Constellation points similar to APSK are directly selected from QAM so that they can maintain low PAPR while ensuring backward

$$s_k = \frac{1}{\sqrt{42}}\{(1-2\boldsymbol{b}_k(0))[4-(1-2\boldsymbol{b}_k(2))[2-(1-2\boldsymbol{b}_k(4))]] + j(1-2\boldsymbol{b}_k(1))[4-(1-2\boldsymbol{b}_k(3))[2-(1-2\boldsymbol{b}_k(5))]]\}. \quad (6)$$

$$s_k = \frac{1}{\sqrt{170}}\{(1-2\boldsymbol{b}_k(0))[8-(1-2\boldsymbol{b}_k(2))[4-(1-2\boldsymbol{b}_k(4))[2-(1-2\boldsymbol{b}_k(6))]]] + j(1-2\boldsymbol{b}_k(1))[8-(1-2\boldsymbol{b}_k(3))[4-(1-2\boldsymbol{b}_k(5))[2-(1-2\boldsymbol{b}_k(7))]]]\}. \quad (7)$$

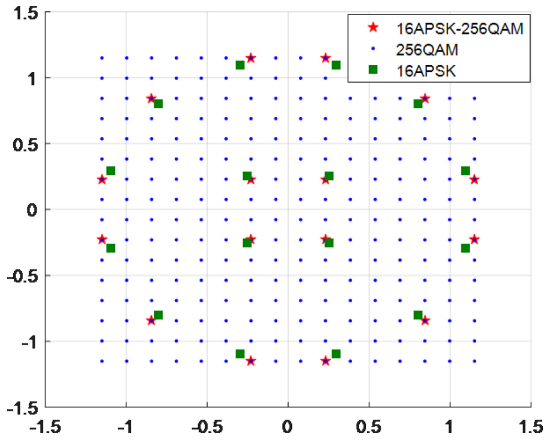

FIGURE 2. The proposed 16APSK_256QAM constellation using projection over QAM.

compatibility. Here, the minimum Euclidean distance criterion is used to select points.

N-APSK and M-QAM constellation sets are represented as C_{APSK} and C_{QAM} respectively:

$$\begin{aligned} C_{APSK} &= \{(x_1, y_1), (x_2, y_2), \ldots, (x_N, y_N)\}, \\ C_{QAM} &= \left\{\left(x'_1, y'_1\right), \left(x'_2, y'_2\right), \ldots, \left(x'_M, y'_M\right)\right\}, \end{aligned} \tag{9}$$

where (x_k, y_k) denotes the horizontal and vertical coordinates of the k-th constellation point on the N-APSK, and (x'_j, y'_j) denotes the horizontal and vertical coordinates of the j-th constellation point on M-QAM.

After the average power normalization of N-APSK and M-QAM constellations, points of N-APSK can be mapped to M-QAM. Specifically, the Euclidean distance $\boldsymbol{d}_k$ between the k-th constellation point of N-APSK and total M QAM constellation points is calculated, where $\boldsymbol{d}_k$ is a matrix of $1 \times M$. The constellation point corresponding to the minimum value in the matrix will be the k-th constellation point of N-APSK_M-QAM. Thus, the horizontal and vertical coordinates of the k-th N-APSK_M-QAM constellation point can be described as:

$$\min_{\left(x'_j, y'_j\right)} d_k = \left(x_k - x'_j\right)^2 + \left(y_k - y'_j\right)^2, j = 1, 2, \ldots, M. \tag{10}$$

Thus, we can search for N non-coincident points in QAM of M points to make up an N-APSK_M-QAM constellation. The example of 16APSK_256QAM is shown in Fig. 2. It can be seen that constellation points of 16APSK_256QAM are all derived from QAM and the diagram is very similar to 16APSK.

B. BIT-TO-SYMBOL MAPPING FOR PSEUDO-APSK CONSTELLATION

Bit-to-symbol mapping rules are essential for systems with encoding and decoding modules and using soft-demodulation algorithms at the receiver. Appropriate mapping rules can improve system performance effectively. This section gives the bit-to-symbol mapping rules for N-APSK_M-QAM constellations.

We multiplex APSK bit-to-symbol mapping rules in DVB standard [37], [38] to design the bit-to-symbol mapping method for N-APSK_M-QAM. Constellation points on M-QAM are considered to be obtained from random n bits, where $n = \log_2 N$. Thus, n bits of $\boldsymbol{e}(0), \boldsymbol{e}(1), \ldots, \boldsymbol{e}(n-1)$ are used to represent m bits, $\boldsymbol{b}(0), \boldsymbol{b}(1), \ldots, \boldsymbol{b}(m-1)$ in the original M-QAM, where $m = \log_2 M$.

In 16APSK_64QAM, symbols of 4 bits on APSK are projected to constellation points of 6 bits on QAM. Thus, we need to construct a 6-bit sequence based on 4 information bits and then select the corresponding point in the original 64QAM. The 4 bits of an APSK symbol are denoted as $\boldsymbol{e}(0)$, $\boldsymbol{e}(1)$, $\boldsymbol{e}(2)$, $\boldsymbol{e}(3)$ and the 6 bits of a QAM symbol are represented as $\boldsymbol{b}(0)$, $\boldsymbol{b}(1)$, $\boldsymbol{b}(2)$, $\boldsymbol{b}(3)$, $\boldsymbol{b}(4)$, $\boldsymbol{b}(5)$. For 16APSK_64QAM based on (4+12)-APSK defined in [37], the mapping rules from $\boldsymbol{e}$ to $\boldsymbol{b}$, i.e., $\boldsymbol{b} = f(\boldsymbol{e})$ are described as

$$\begin{cases} \boldsymbol{b}(0) = \boldsymbol{e}(2) \\ \boldsymbol{b}(1) = \boldsymbol{e}(3) \\ \boldsymbol{b}(2) = \widetilde{\boldsymbol{e}}(0) \\ \boldsymbol{b}(3) = \widetilde{\boldsymbol{e}}(1) \\ \boldsymbol{b}(4) = \boldsymbol{e}(0) \vee \boldsymbol{e}(1) \\ \boldsymbol{b}(5) = \boldsymbol{e}(0) \vee \boldsymbol{e}(1) \end{cases}, \tag{11}$$

where $\sim$ represents the logical operator "non", and $\vee$ represents the logical operator "or". By taking (11) into (6), bit-to-symbol mapping rules of 16APSK_64QAM can be expressed as (12), shown at the bottom of the page. Accordingly, the bit-to-symbol mapping table is presented in Fig. 3.

Similarly, in 16APSK_256QAM, symbols of 4 bits on APSK are projected to constellation points of 8 bits on QAM. Thus, we need to construct an 8-bit sequence based on 4 information bits and then select the corresponding point in 256QAM. The 4 bits of an APSK symbol are denoted as $\boldsymbol{e}(0)$, $\boldsymbol{e}(1)$, $\boldsymbol{e}(2)$, $\boldsymbol{e}(3)$ and the 8 bits of a QAM symbol are represented as $\boldsymbol{b}(0)$, $\boldsymbol{b}(1)$,..., $\boldsymbol{b}(7)$. For 16APSK_64QAM based on (4+12)-APSK defined in [37], the mapping rules from $\boldsymbol{e}$ to $\boldsymbol{b}$, i.e., $\boldsymbol{b} = f(\boldsymbol{e})$ are described as

$$\begin{cases} \boldsymbol{b}(0) = \boldsymbol{e}(2) \\ \boldsymbol{b}(1) = \boldsymbol{e}(3) \\ \boldsymbol{b}(2) = \widetilde{\boldsymbol{e}}(0) \\ \boldsymbol{b}(3) = \widetilde{\boldsymbol{e}}(1) \\ \boldsymbol{b}(4) = \boldsymbol{e}(0) \vee \boldsymbol{e}(1) \\ \boldsymbol{b}(5) = \boldsymbol{e}(0) \vee \boldsymbol{e}(1) \\ \boldsymbol{b}(6) = \widetilde{\boldsymbol{e}}(0) \wedge \left(\boldsymbol{e}(0) \bigoplus \boldsymbol{e}(1)\right) \\ \boldsymbol{b}(7) = \widetilde{\boldsymbol{e}}(1) \wedge \left(\boldsymbol{e}(0) \bigoplus \boldsymbol{e}(1)\right) \end{cases}, \tag{13}$$

where $\wedge$ represents the logical operator "and", and $\bigoplus$ denotes the logical operator "XOR". By taking (13) into (7),

$$\begin{aligned} s = \frac{1}{\sqrt{42}}\{&(1 - 2\boldsymbol{e}(2))[4 - (1 - 2\widetilde{\boldsymbol{e}}(0))[2 - (1 - 2(\boldsymbol{e}(0) \vee \boldsymbol{e}(1)))]] \\ &+ j(1 - 2\boldsymbol{e}(3))[4 - (1 - 2\widetilde{\boldsymbol{e}}(1))[2 - (1 - 2(\boldsymbol{e}(0) \vee \boldsymbol{e}(1)))]]\}. \end{aligned} \tag{12}$$

Index	Bits $e(0)$-$e(3)$	*Bits(64QAM) $b(0)$-$b(5)$	Symbol s	Index	Bits $e(0)$-$e(3)$	*Bits(64QAM) $b(0)$-$b(5)$	Symbol s
1	1100	000011	$\frac{1}{\sqrt{42}}(1+1i)$	9	0010	101100	$\frac{1}{\sqrt{42}}(-5+5i)$
2	1110	100011	$\frac{1}{\sqrt{42}}(-1+1i)$	10	0110	101011	$\frac{1}{\sqrt{42}}(-7+1i)$
3	1111	110011	$\frac{1}{\sqrt{42}}(-1-1i)$	11	0111	111011	$\frac{1}{\sqrt{42}}(-7-1i)$
4	1101	010011	$\frac{1}{\sqrt{42}}(1-1i)$	12	0011	111100	$\frac{1}{\sqrt{42}}(-5-5i)$
5	0100	001011	$\frac{1}{\sqrt{42}}(7+1i)$	13	1011	110111	$\frac{1}{\sqrt{42}}(-1-7i)$
6	0000	001100	$\frac{1}{\sqrt{42}}(5+5i)$	14	1001	010111	$\frac{1}{\sqrt{42}}(1-7i)$
7	1000	000111	$\frac{1}{\sqrt{42}}(1+7i)$	15	0001	011100	$\frac{1}{\sqrt{42}}(5-5i)$
8	1010	100111	$\frac{1}{\sqrt{42}}(-1+7i)$	16	0101	011011	$\frac{1}{\sqrt{42}}(7-1i)$

* red: $\boldsymbol{b}(0)=\boldsymbol{e}(2)$; blue: $\boldsymbol{b}(1)=\boldsymbol{e}(3)$; green: $\boldsymbol{b}(2)=\tilde{\boldsymbol{e}}(0)$; black: $\boldsymbol{b}(3)=\tilde{\boldsymbol{e}}(1)$; gray: $\boldsymbol{b}(4)=\boldsymbol{b}(5)=\boldsymbol{e}(0)\vee\boldsymbol{e}(1)$

FIGURE 3. The bit-to-symbol mapping table of proposed 16APSK_64QAM constellation using projection over QAM.

Index	Bits $e(0)$-$e(3)$	*Bits(256QAM) $b(0)$-$b(7)$	Symbol s	Index	Bits $e(0)$-$e(3)$	*Bits(256QAM) $b(0)$-$b(7)$	Symbol s
1	1100	00001100	$\frac{1}{\sqrt{170}}(3+3i)$	9	0010	10110000	$\frac{1}{\sqrt{170}}(-11+11i)$
2	1110	10001100	$\frac{1}{\sqrt{170}}(-3+3i)$	10	0110	10101110	$\frac{1}{\sqrt{170}}(-15+3i)$
3	1111	11001100	$\frac{1}{\sqrt{170}}(-3-3i)$	11	0111	11101110	$\frac{1}{\sqrt{170}}(-15-3i)$
4	1101	01001100	$\frac{1}{\sqrt{170}}(3-3i)$	12	0011	11110000	$\frac{1}{\sqrt{170}}(-11-11i)$
5	0100	00101110	$\frac{1}{\sqrt{170}}(15+3i)$	13	1011	11011101	$\frac{1}{\sqrt{170}}(-3-15i)$
6	0000	00110000	$\frac{1}{\sqrt{170}}(11+11i)$	14	1001	01011101	$\frac{1}{\sqrt{170}}(3-15i)$
7	1000	00011101	$\frac{1}{\sqrt{170}}(3+15i)$	15	0001	01110000	$\frac{1}{\sqrt{170}}(11-11i)$
8	1010	10011101	$\frac{1}{\sqrt{170}}(-3+15i)$	16	0101	01101110	$\frac{1}{\sqrt{170}}(15-3i)$

*red: $\boldsymbol{b}(0)=\boldsymbol{e}(2)$; blue: $\boldsymbol{b}(1)=\boldsymbol{e}(3)$; green: $\boldsymbol{b}(2)=\tilde{\boldsymbol{e}}(0)$; black: $\boldsymbol{b}(3)=\tilde{\boldsymbol{e}}(1)$; orange: $\boldsymbol{b}(4)=\boldsymbol{b}(5)=\boldsymbol{e}(0)\vee\boldsymbol{e}(1)$; pink: $\boldsymbol{b}(6)=\tilde{\boldsymbol{e}}(0)\wedge(\boldsymbol{e}(0)\oplus\boldsymbol{e}(1))$; purple: $\boldsymbol{b}(7)=\tilde{\boldsymbol{e}}(1)\wedge(\boldsymbol{e}(0)\oplus\boldsymbol{e}(1))$

FIGURE 4. The bit-to-symbol mapping table of proposed 16APSK_256QAM constellation using projection over QAM.

bit-to-symbol mapping rules of 16APSK_256QAM can be expressed as (14), shown at the bottom of the page. Besides, the corresponding bit-to-symbol mapping table is presented in Fig. 4.

The bit-to-symbol mapping rules of 32APSK_256QAM and 64APSK_256QAM are respectively designed based on the mapping rules of 32APSK and 64APSK in DVB standard [37], [38]. For example, the bit-to-symbol mapping table of 32APSK_256QAM based on (4+12+16)-APSK in [38] is shown as Table 2 in Appendix.

IV. CONSTELLATION DESIGN OF QAM-COMPATIBLE PSEUDO-SPIRAL

Based on the proposed design concept, in this section, we provide an example of NR-compatible pseudo-Spiral constellation design to combat phase noise.

A. DESIGN PROCESS OF PSEUDO-SPIRAL

PN causes constellation points to rotate and shift, and it affects more severely symbols with higher magnitudes. Existing research has proposed spiral constellations of simple design to combat PN, in which the density of points near the origin is high and gets lower outward [30]. However, the spiral does not have compatibility, which hinders its practical application. Therefore, in this section, N-order pSpiral points are selected from M-order QAM to keep phase noise resistance while ensuring backward compatibility with NR.

The process of N-Spiral_M-QAM constellation design is summarized as three steps below:

- First, an M-order QAM constellation is picked according to the modulation mapper specified in 3GPP TS 38.211 [5].
- Second, a spiral constellation of N points is generated according to the proposed method in [30].
- Finally, we project the spiral over QAM to get an N-Spiral_M-QAM constellation. By using the method of exhaustive search, the constellation points of N-Spiral and M-QAM are compared one by one. Different from the principle of minimum Euclidean distance used to select pAPSK points, we propose minimum radial and angular weighted distance considering PN to find N

$$s=\frac{1}{\sqrt{170}}\Big\{(1-2\boldsymbol{e}(2))\Big[8-(1-2\tilde{\boldsymbol{e}}(0))\Big[4-(1-2(\boldsymbol{e}(0)\vee\boldsymbol{e}(1)))\Big[2-\Big(1-2\Big(\tilde{\boldsymbol{e}}(0)\wedge\Big(\boldsymbol{e}(0)\bigoplus\boldsymbol{e}(1)\Big)\Big)\Big)\Big]\Big]\Big] \\ +j(1-2\boldsymbol{e}(3))\Big[8-(1-2\tilde{\boldsymbol{e}}(1))\Big[4-(1-2(\boldsymbol{e}(0)\vee\boldsymbol{e}(1)))\Big[2-\Big(1-2\Big(\tilde{\boldsymbol{e}}(1)\wedge\Big(\boldsymbol{e}(0)\bigoplus\boldsymbol{e}(1)\Big)\Big)\Big)\Big]\Big]\Big]\Big\}. \tag{14}$$

non-coincident points of M-QAM similar to the original N-Spiral.

For the second step, according to [30], the spiral constellation points are placed along the Archimedean spiral based on the following rule,

$$c_n = t_n e^{jt_n} n = 1, \ldots, N, \tag{15}$$

where N is the modulation order of the desired constellation and $t_1 < t_2 < \cdots < t_N$. After derivation and solving considering AWGN channel with PN in [30], t_n is defined by

$$t_n^2 = \frac{(4\pi n)^2 f_s}{2} + \sqrt{\frac{(4\pi n)^4 f_s^2}{4} + (4\pi n)^2}, \tag{16}$$

where the spiral shape parameter f_s is determined by the channel conditions, such as a possible value of $f_s = \frac{2\sigma_\phi^2}{\sigma_n^2}$. Furthermore, it is also observed in [30] that better performance can be achieved to choose the optimal value of f_s as

$$f_s^* = arg \max_{f_s} I_{f_s}(\mathbf{x}; \mathbf{y}), \tag{17}$$

where I_{f_s} is the bound on the achievable IR, which represents a lower bound to the channel capacity. Specifically, I_{f_s} can be computed as

$$I_{f_s}(\mathbf{x}; \mathbf{y}) = \lim_{L \to \infty} \frac{1}{L} \mathrm{E}\left[\log_2 \frac{p(\mathbf{y}|\mathbf{x})}{\sum_{\mathbf{x}'} p(\mathbf{y}|\mathbf{x}')P(\mathbf{x}')}\right], \tag{18}$$

where $\mathbf{x}$ is a sequence of L transmitted symbols and $\mathbf{y}$ represents the corresponding received ones. The probability density function (PDF) of the selected auxiliary channel law is defined by $p(\mathbf{y}|\mathbf{x})$ and the probability distribution of the transmitted symbols is defined by $P(\mathbf{x}')$.

To narrow down the search scope, a set of possible values of f_s can be obtained through the following equation in [30],

$$f_s = \frac{1}{(2M_{out} + 1)^2}, \tag{19}$$

where M_{out} is the number of points on the outermost lap of the spiral. For instance, for $M_{out} \in [8, 15]$, good values of f_s are calculated as the set $[3.46, 2.77, 2.27, 1.89, 1.60, 1.37, 1.19, 1.04] \times 10^{-3}$. Subsequently, by fine-tuning these values, the maximum IR can be achieved. Note that when $f_s = 0$, the spiral constellation optimized for the AWGN channel is obtained. Finally, the constellation points are normalized to ensure the spiral constellation has unitary average power.

In the last step, the constellation points similar to N-Spiral are then selected from M-QAM so that they can acquire backward compatibility while maintaining phase noise resistance. Particularly, instead of the minimum Euclidean distance criterion, the principle of minimum radial and angular weighted distance is proposed below to select points. This is because the minimum angular distance between constellation points on the outer laps is more important than the minimum Euclidean distance in the presence of phase noise.

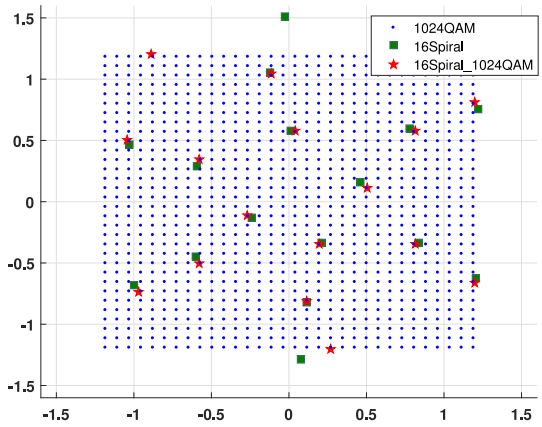

FIGURE 5. 16Spiral_1024QAM constellation for PN variance $\sigma_\phi^2 = 0.04$ using projection over QAM. The Spiral parameter $f_s = 0.00794$, and the weighted factors are $\alpha = 0.91$, $\beta = 0.09$ respectively.

N-Spiral and M-QAM constellation sets are represented as C_{Spiral} and C_{QAM} respectively:

$$\begin{aligned} C_{Spiral} &= \{(\rho_1, \theta_1), (\rho_2, \theta_2), \ldots, (\rho_N, \theta_N)\}, \\ C_{QAM} &= \left\{\left(\rho_1', \theta_1'\right), \left(\rho_2', \theta_2'\right), \ldots, \left(\rho_M', \theta_M'\right)\right\}, \end{aligned} \tag{20}$$

where (ρ_k, θ_k) denotes the amplitude and phase of the k-th constellation point on N-Spiral, and (ρ_j', θ_j') denotes the amplitude and phase of the j-th constellation point on M-QAM. After the average power normalization of N-Spiral and M-QAM constellations respectively, points of N-Spiral are mapped to M-QAM. The radial and angular distance $\Delta\rho$ and $\Delta\theta$ between the k-th constellation point of N-Spiral and the j-th point of M-QAM are calculated as

$$\begin{aligned} \Delta\rho_{kj} &= |\rho_k - \rho_j'|, \\ \Delta\theta_{kj} &= |\theta_k - \theta_j'|. \end{aligned} \tag{21}$$

Then, N non-coincident points in QAM are selected to form N-Spiral_M-QAM constellation by exhaustive search with the principle of minimum radial and angular weighted distance, which can be expressed as

$$\min_{\left(\rho_j', \theta_j'\right)} f\left(\Delta\rho_{kj}, \Delta\theta_{kj}\right) = \alpha \cdot \left(\Delta\rho_{kj}\right)^2 + \beta \cdot \left(\Delta\theta_{kj}\right)^2, \tag{22}$$

where the values of parameter α and β are related to Gaussian noise and phase noise. Specifically, we set $\alpha + \beta = 1$, and search for the pair (α, β) to achieve the best performance of N-Spiral_M-QAM under given conditions using exhaustive search.

Thus, the parameter f_s of Spiral is optimized first, and the optimization of the weighted factors (α, β) is then performed when phase noise changes to obtain better PN resistance of pSpiral compatible with QAM. For example, the 16Spiral_1024QAM constellation diagram is shown in Fig. 5. It can be seen that constellation points of

TABLE 1. Simulation settings.

Parameters	Assumptions
Modulation schemes	16QAM, 16APSK_256QAM, 64QAM, 64Spiral, 64Spiral_1024QAM
PN variance σ_ϕ^2	0.01, 0.04, 0.08
Carrier frequency	70 GHz
Subcarrier spacing (SCS)	960 kHz
Allocated subcarriers (DFT size)	480, 792, 960
FFT size	1024
Cyclic Prefix (CP) length	72
PA model	CMOS
Input Backoff IBO	0, 2, 4 dB
Channel	AWGN
Channel estimation	MMSE
Channel coding	LDPC
Code rate R	490/1024, 569/1024, 751/1024
Waveform	DFT-s-OFDM

16Spiral_1024QAM are all derived from QAM and form a similar shape of the spiral.

B. BIT-TO-SYMBOL MAPPING FOR PSEUDO-SPIRAL CONSTELLATION

As previously mentioned, phase noise leads to the rotation of constellation points. Therefore, we utilize Gray code for bit-to-symbol mapping of N-Spiral_M-QAM considering the closest points affected by phase noise, which satisfies only one-bit difference between adjacent constellation points on the original spiral line. For example, the bit-to-symbol mapping table of 16-Spiral_1024-QAM for PN variance 0.08 is given in Table 3 in Appendix.

V. SIMULATION RESULTS

In this section, we present simulation results to evaluate the performance of the proposed constellation design method using projection over QAM. First, the BLER performance of 16-APSK_256-QAM for coded systems is simulated and compared with QAM under different code rates and allocated subcarriers. Then, the SER performance of 64-Spiral_1024-QAM under different PN variances for uncoded systems is evaluated and compared with QAM, Spiral, as well as the constellation selected by minimum Euclidean distance. Besides, the spectral efficiency (SE) curves of the proposed pSpiral are also presented to demonstrate its robustness to PN.

Simulation parameters are summarized in Table 1, which are selected based on the typical high-frequency scenarios considered in 5G communication. In particular, a carrier frequency of 70 GHz within the millimeter-wave frequency range and a subcarrier spacing of 960 kHz are selected, where hardware impairments including phase noise and PA nonlinearity are considered [42].

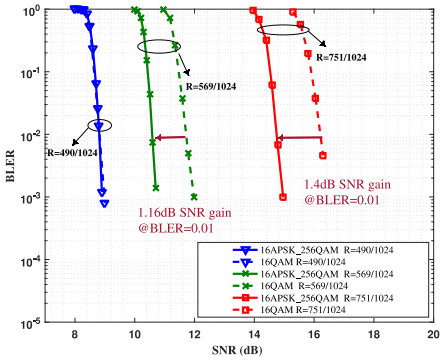

FIGURE 6. BLER performance of proposed 16-APSK_256-QAM compared to 16QAM with different code rates and 792 subcarriers.

A. PERFORMANCE EVALUATION OF 16-APSK_256-QAM

The simulation in this part is performed based on Discrete Fourier Transform-Spread-Orthogonal Frequency Division Multiplexing (DFT-s-OFDM) waveform with a low-density parity-check (LDPC) coded system. The AWGN channel is considered, along with the nonlinear distortion caused by the CMOS power amplifier modeled as (2) and (3). The simulation parameter settings are as shown in Table 1. Transmission signals x_n are equally sent, and received signals y_n are obtained after passing through the power amplifier and AWGN channel. The hard decision demodulation algorithm directly judges based on the amplitude and phase of the received signal, and needs to store the lookup table in advance to determine the corresponding bits of a constellation point. Therefore, we use the Maximum Logarithm Maximum A Posteriori (Max-Log-MAP) soft decision demodulation algorithm at the receiver instead, which is based on the Log-Likelihood ratio (LLR) algorithm.

Fig. 6 shows the BLER performance of proposed 16-APSK_256-QAM compared to 16QAM at different code rates. The number of subcarriers is set to 792 and there is no input back-off (IBO). With the fixed number of transmission bits, we simulate the BLER of 16-APSK_256-QAM and 16QAM at three code rates: 490/1024, 569/1024, and 751/1024. As shown in Fig. 6, when the code rate is low, i.e., $R = 490/1024$, the performance of 16APSK_256QAM and 16QAM is similar. However, the SNR gain of 16APSK_256 QAM over 16QAM increases to more than 1 dB with higher code rates, as the nonlinear distortion of the PA has a greater impact on system performance at high code rates which has weaker error correction ability, and the low PAPR characteristic of 16APSK_256 QAM can help it combat the nonlinear distortion. Specifically, when BLER reaches 0.01, there are 1.16 dB and 1.4dB SNR gains at the code rates of 569/1024 and 751/1024, respectively. Therefore, it can be concluded that in scenarios with better wireless link quality where medium-to-high code rates are required, 16APSK_256QAM can be an effective constellation modulation alternative to improve the reliability of the system.

The BLER performance of proposed 16-APSK_256-QAM compared to 16QAM with the different number

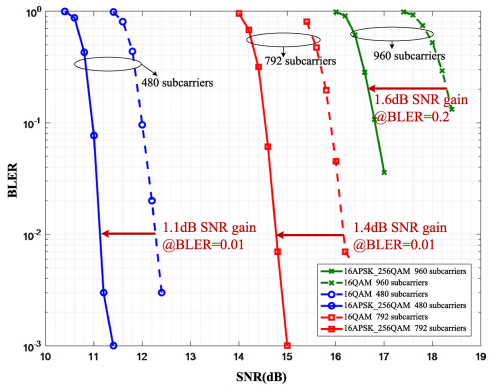

FIGURE 7. BLER performance of proposed 16-APSK_256-QAM compared to 16QAM with the different number of subcarriers at the code rate $R = 751/1024$.

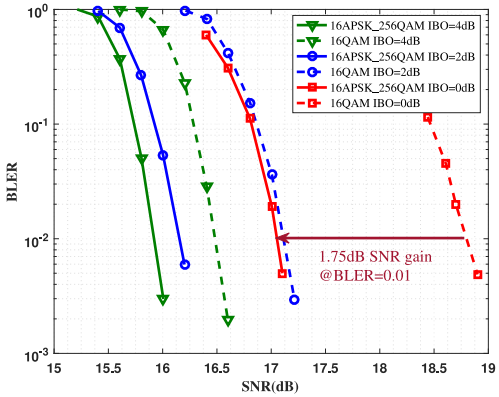

FIGURE 8. BLER performance of proposed 16-APSK_256-QAM compared to 16QAM with different IBO values and 960 subcarriers at $R = 751/1024$.

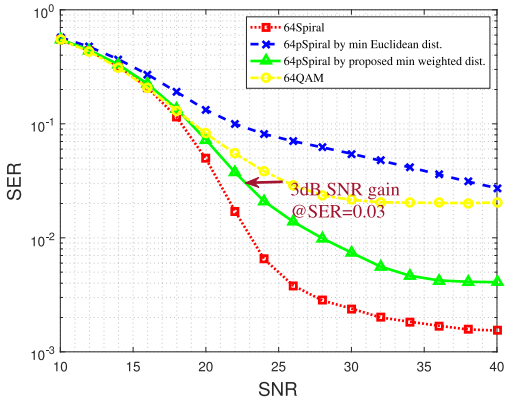

FIGURE 9. SER performance of proposed 64-Spiral_1024-QAM when PN variance is 0.01. The Spiral parameter $f_s = 0.00352$, and the weighted factors are $\alpha = 0.88$, $\beta = 0.12$ respectively.

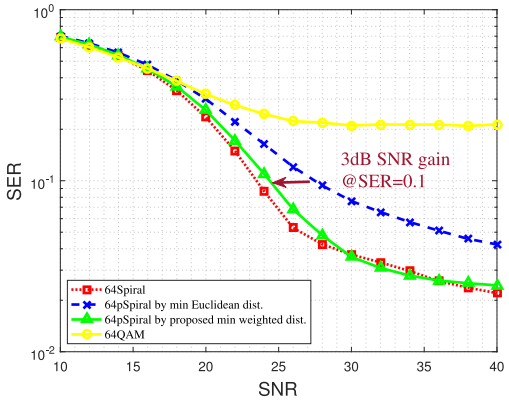

FIGURE 10. SER performance of proposed 64-Spiral_1024-QAM when PN variance is 0.08. The Spiral parameter $f_s = 0.01065$, and the weighted factors are $\alpha = 0.92$, $\beta = 0.08$ respectively.

of subcarriers is presented in Fig. 7, at the code rate $R = 751/1024$ and without IBO. The simulation results show that as the number of subcarriers increases, the performance of the overall system deteriorates. This is because more subcarriers lead to higher PAPR of the system, and as a result, more signals enter the non-linear region. For a specific number of subcarriers, we can notice that 16APSK_256QAM outperforms 16QAM thanks to its lower PAPR, and the gains enlarge with more subcarriers. Specifically, the SNR gains of the proposed constellation compared to QAM when BLER is 0.01 are 1.1 dB, 1.4 dB and 1.8 dB for 480, 792 and 960 subcarriers, respectively.

Fig. 8 compares the BLER performance of proposed 16-APSK_256-QAM and 16QAM under different IBO values. The number of subcarriers is set to 960, and the results are obtained at the code rate $R = 751/1024$. As the IBO value increases, more signals enter the linear region, resulting in a lower SNR required for the system and an effective improvement in performance for both 16APSK_256QAM and 16QAM. However, under the same SNR value, the BLER of 16APSK_256QAM at $IBO = 2$ dB (marked by blue circle solid curve) is much lower than that of 16QAM at $IBO = 4$ dB (marked by green triangle dashed curve). Higher IBO values mean lower power efficiency. Therefore, 16APSK_256QAM requires less power consumption than 16QAM to achieve the same BLER performance, which is more conducive to energy-saving transmission. In particular, the performance gains of 16APSK_256QAM compared to 16QAM are 1.75 dB, 0.96 dB and 0.56 dB respectively for IBO values 0, 2, and 4 dB, when BLER reaches 0.01. Moreover, the BLER gap between 16APSK_256QAM and 16QAM narrows down with the increasing IBO values, in that the effect of PA nonlinearity becomes weaker, and the advantage of the low PAPR 16APSK_256QAM gets less obvious. Considering that the practical system cannot increase the IBO value without limitation to achieve excellent performance, which sacrifices power efficiency, 16APSK_256QAM achieves a compromise between power consumption and the ability to resist PA nonlinearity.

B. PERFORMANCE EVALUATION OF 64-SPIRAL_1024-QAM

In this subsection, we consider an AWGN channel with PN. For the signal model defined in (4), we adopt the detector in [30] to perform demodulation, which is derived based on the low PN and a high SNR approximation. The likelihood function of the k-th received symbol y_k and the transmitted

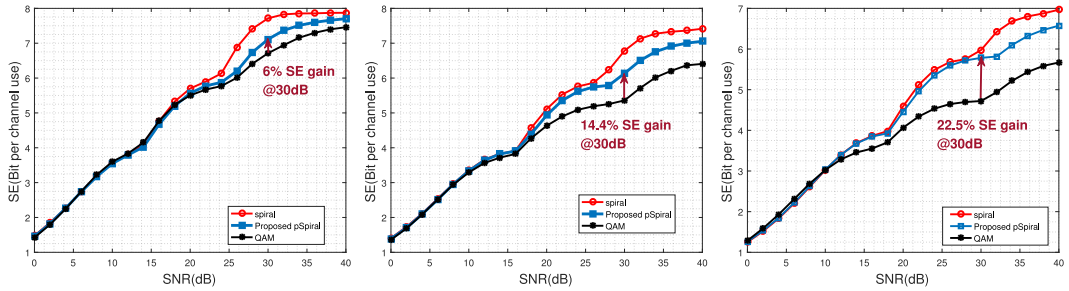

(a) SE for PN variance 0.01. (b) SE for PN variance 0.04. (c) SE for PN variance 0.08.

FIGURE 11. The SE performance of the proposed pSpiral compared with QAM and Spiral for different PN variances.

TABLE 2. The bit-to-symbol mapping table of proposed 32APSK_256QAM constellation.

Index	Bits	Bits(256QAM)	Symbol	Index	Bits	Bits(256QAM)	Symbol
1	01111	00001100	$\frac{1}{\sqrt{170}}(3+3i)$	17	01011	00101110	$\frac{1}{\sqrt{170}}(15+3i)$
2	01101	10001100	$\frac{1}{\sqrt{170}}(-3+3i)$	18	01010	00111001	$\frac{1}{\sqrt{170}}(13+9i)$
3	11101	11001100	$\frac{1}{\sqrt{170}}(-3-3i)$	19	00010	00110110	$\frac{1}{\sqrt{170}}(9+13i)$
4	11111	01001100	$\frac{1}{\sqrt{170}}(3-3i)$	20	00011	00011101	$\frac{1}{\sqrt{170}}(3+15i)$
5	01110	00100110	$\frac{1}{\sqrt{170}}(9+3i)$	21	00001	10011101	$\frac{1}{\sqrt{170}}(-3+15i)$
6	00110	00000011	$\frac{1}{\sqrt{170}}(7+7i)$	22	00000	10110110	$\frac{1}{\sqrt{170}}(-9+13i)$
7	00111	00011001	$\frac{1}{\sqrt{170}}(3+9i)$	23	01000	10111001	$\frac{1}{\sqrt{170}}(-13+9i)$
8	00101	10011001	$\frac{1}{\sqrt{170}}(-3+9i)$	24	01001	10101110	$\frac{1}{\sqrt{170}}(-15+3i)$
9	00100	10000011	$\frac{1}{\sqrt{170}}(-7+7i)$	25	11001	11101110	$\frac{1}{\sqrt{170}}(-15-3i)$
10	01100	10100110	$\frac{1}{\sqrt{170}}(-9+3i)$	26	11000	11111001	$\frac{1}{\sqrt{170}}(-13-9i)$
11	11100	11100110	$\frac{1}{\sqrt{170}}(-9-3i)$	27	10000	11110110	$\frac{1}{\sqrt{170}}(-9-13i)$
12	10100	11000011	$\frac{1}{\sqrt{170}}(-7-7i)$	28	10001	11011101	$\frac{1}{\sqrt{170}}(-3-15i)$
13	10101	11011001	$\frac{1}{\sqrt{170}}(-3-9i)$	29	10011	01011101	$\frac{1}{\sqrt{170}}(3-15i)$
14	10111	01011001	$\frac{1}{\sqrt{170}}(3-9i)$	30	10010	01110110	$\frac{1}{\sqrt{170}}(9-13i)$
15	10110	01000011	$\frac{1}{\sqrt{170}}(7-7i)$	31	11010	01111001	$\frac{1}{\sqrt{170}}(13-9i)$
16	11110	01100110	$\frac{1}{\sqrt{170}}(9-3i)$	32	11011	01101110	$\frac{1}{\sqrt{170}}(15-3i)$

symbol x_k is expressed as a Gaussian PDF of two auxiliary variables u_k and v_k to perform detection [30].

We present the uncoded SER performance of the proposed 64-Spiral_1024-QAM constellations compared with 64QAM, 64Spiral and 64-Spiral_1024-QAM selected by minimum Euclidean distance criterion under different PN variances in Fig. 9 and Fig. 10.

For PN variance $\sigma_\phi^2 = 0.01$, the spiral parameter $f_s = 0.00352$ and weighted factors $(\alpha, \beta) = (0.88, 0.12)$, 64-Spiral_1024-QAM (green line) has about 3 dB SNR gain over 64QAM (yellow line) when SER is 0.03 as shown in Fig. 9. In addition, the selected pseudo-spiral constellation using the minimum Euclidean distance criterion (blue line) provides the worst performance here, which indicates that

TABLE 3. The bit-to-symbol mapping table of proposed 16Spiral_1024QAM constellation for PN variance 0.08.

Index	Bits	Bits(1024QAM)	Symbol	Index	Bits	Bits(1024QAM)	Symbol
1	0000	0110110010	$\frac{1}{\sqrt{678}}(-5-3i)$	9	1100	0011011001	$\frac{1}{\sqrt{678}}(-19-17i)$
2	0001	1001110011	$\frac{1}{\sqrt{678}}(7-5i)$	10	1101	1100111011	$\frac{1}{\sqrt{678}}(19-21i)$
3	0011	1001101100	$\frac{1}{\sqrt{678}}(7+9i)$	11	1111	1101000111	$\frac{1}{\sqrt{678}}(21+19i)$
4	0010	0101101101	$\frac{1}{\sqrt{678}}(-9+7i)$	12	1110	0010100101	$\frac{1}{\sqrt{678}}(-21+23i)$
5	0110	0101110110	$\frac{1}{\sqrt{678}}(-9-11i)$	13	1010	0001111101	$\frac{1}{\sqrt{678}}(-25-25i)$
6	0111	1011010110	$\frac{1}{\sqrt{678}}(13-11i)$	14	1011	1110111101	$\frac{1}{\sqrt{678}}(27-25i)$
7	0101	1011101001	$\frac{1}{\sqrt{678}}(15+15i)$	15	1001	1110100010	$\frac{1}{\sqrt{678}}(27+29i)$
8	0100	0100001001	$\frac{1}{\sqrt{678}}(-15+15i)$	16	1000	0000000011	$\frac{1}{\sqrt{678}}(-31+27i)$

the criterion is not applicable in PN environments and that considering the angular distance is necessary.

For larger PN variance $\sigma_\phi^2 = 0.08$, 64QAM reaches an error floor when SER is 0.2, while proposed 64-Spiral_1024-QAM (green line) with the spiral parameter $f_s = 0.01065$ and weighted factors $(\alpha, \beta) = (0.92, 0.08)$ reduces the error floor to near 0.02, which is close to that of original 64Spiral as shown in Fig. 10. Additionally, 64-Spiral_1024-QAM selected with minimum weighted distance (green line) outperforms the one with minimum Euclidean distance (blue line) of about 3 dB when SER is 0.1. This proves the advantage of constellation projection by the proposed minimum radial and angular weighted distance in the presence of PN. For other PN variances and modulation order $N = 16, 256$, the proposed pSpiral constellations are also proved to be superior to QAM in SER performance.

In the end, in Fig. 11, the SE curves of the proposed pSpiral, QAM and Spiral are compared. We can see that as the phase noise variance increases, the performance gain of pSpiral over QAM becomes more significant. This phenomenon demonstrates the advantage of the pSpiral in combating phase noise while remaining compatible with QAM. In particular, the SE of pSpiral outperforms QAM of 22.5% at 30dB for PN variance $\sigma_\phi^2 = 0.08$. Besides, the performance of pSpiral is less affected by phase noise change than QAM, which shows the robustness of the proposed pSpiral. The simulation results also indicate that the Spiral and proposed pSpiral exhibit similar SE performance at moderate to low SNR. This can be attributed to the combined influence of Gaussian noise and phase noise on the transmitted signals at moderate to low SNR levels. The appropriate minimum Euclidean distance of pSpiral and its spiral-like shape enable it to achieve the SE performance close to that of Spiral. Additionally, the Spiral outperforms pSpiral at high SNR levels, where phase noise becomes the predominant factor affecting the performance. The distortion introduced during the projection process for pSpiral results in a performance loss of no more than 0.65 bits per channel use compared to Spiral.

VI. CONCLUSION

This paper has proposed an NR-compatible constellation design method using projection over QAM. Specifically, N-APSK_M-QAM and N-Spiral_M-QAM constellations are given as two examples to illustrate the method. The projection of APSK and Spiral constellations is based on the minimum Euclidean distance and the proposed minimum weighted radial-angular distance criteria, respectively. Simulation results demonstrate that the proposed pAPSK modulation scheme outperforms QAM by more than 1 dB SNR gain at medium-to-high code rates in the presence of nonlinear distortion caused by the power amplifier. Furthermore, the proposed pSpiral constellations show improved error rate performance under PN conditions and enhanced robustness to PN compared with QAM. Moreover, the SNR gain achieved by pSpiral over QAM reaches 3 dB.

Consequently, the proposed modulation method using projection over QAM not only ensures compatibility with NR but also preserves the advantages of the original constellations, providing a straightforward and effective unified constellation design framework for future B5G/6G systems. By applying this method, other NR-compatible constellations resistant to non-ideal factors can also be obtained, such as constellations that simultaneously combat PA nonlinearity and PN, or constellations that mitigate IQ imbalance.

APPENDIX

The bit-to-symbol mapping table of 32APSK_256QAM based on (4+12+16)-APSK, and the bit-to-symbol mapping table of 16-Spiral_1024-QAM for PN variance 0.08 are given in Table 2 and Table 3 respectively.

REFERENCES

[1] D. Soldani, "6G fundamentals: Vision and enabling technologies: From 5G to 6G trustworthy and resilient systems," *J. Telecommun. Digit. Econ.*, vol. 9, no. 3, pp. 58–86, 2021.

[2] W. Jiang, B. Han, M. A. Habibi, and H. D. Schotten, "The road towards 6G: A comprehensive survey," *IEEE Open J. Commun. Soc.*, vol. 2, pp. 334–366, 2021.

[3] S. He et al., "A survey of millimeter-wave communication: Physical-layer technology specifications and enabling transmission technologies," *Proc. IEEE*, vol. 109, no. 10, pp. 1666–1705, Oct. 2021.

[4] A. N. Uwaechia and N. M. Mahyuddin, "A comprehensive survey on millimeter wave communications for fifth-generation wireless networks: Feasibility and challenges," *IEEE Access*, vol. 8, pp. 62367–62414, 2020.

[5] "3rd generation partnership project; technical specification group radio access network; NR; physical channels and modulation (Release 17)," 3GPP, Sophia Antipolis, France, 3GPP Rep. TS 38.211, version 17.4.0, Dec. 2022.

[6] Q. Ouyang, N. Ye, J. Gao, A. Wang, and L. Zhao, "Joint in-orbit computation and communication for minimizing download time from LEO satellites," *IEEE Trans. Mobile Comput.*, early access, Jun. 2, 2023, doi: 10.1109/TMC.2023.3282243.

[7] J. Pan et al., "AI-driven blind signature classification for IoT connectivity: A deep learning approach," *IEEE Trans. Wireless Commun.*, vol. 21, no. 8, pp. 6033–6047, Aug. 2022.

[8] J. Tellado, "Peak to average power reduction for multicarrier modulation," Ph.D. dissertation, Dept. Elect. Eng., Stanford Univ., Stanford, CA, USA, 2000

[9] B. Krongold and D. Jones, "PAR reduction in OFDM via active constellation extension," *IEEE Trans. Broadcast.*, vol. 49, no. 3, pp. 258–268, Sep. 2003.

[10] Y. Rahmatallah and S. Mohan, "Peak-to-average power ratio reduction in OFDM systems: A survey and taxonomy," *IEEE Commun. Surveys Tuts.*, vol. 15, no. 4, pp. 1567–1592, 1st Quart., 2013.

[11] Y. Kou, W.-S. Lu, and A. Antoniou, "New peak-to-average power-ratio reduction algorithms for multicarrier communications," *IEEE Trans. Circuits Syst. I, Reg. Papers*, vol. 51, no. 9, pp. 1790–1800, Sep. 2004.

[12] M. Sharif and B. Hassibi, "A deterministic algorithm that achieves the PMEPR of c log n for multicarrier signals," in *Proc. IEEE Int. Conf. Acoust. Speech Signal Process. (ICASSP).*, vol. 4, 2003, pp. 540–543.

[13] Y. J. Kou, W.-S. Lu, and A. Antoniou, "A new peak-to-average power-ratio reduction algorithm for OFDM systems via constellation extension," *IEEE Trans. Wireless Commun.*, vol. 6, no. 5, pp. 1823–1832, May 2007.

[14] Y. Shi, D. He, W. Huang, Y. Xu, Y. Guan, and J. Sun, "Constellation shifting based on QAM with gray coding for PAPR reduction of OFDM systems," in *Proc. IEEE Int. Symp. Broadband Multimedia Syst. Broadcast. (BMSB)*, 2013, pp. 1–3.

[15] J. Zhang, T. Wang, and X. Zhou, "A PAPR reduction method for OFDM systems," *Telecommun. Eng.*, vol. 48, no. 4, pp. 27–29, 2008.

[16] C. Thomas, M. Weidner, and S. Durrani, "Digital amplitude-phase keying with M-ary alphabets," *IEEE Trans. Commun.*, vol. 22, no. 2, pp. 168–180, Feb. 1974.

[17] Z. Liu, Q. Xie, K. Peng, and Z. Yang, "APSK constellation with gray mapping," *IEEE Commun. Lett.*, vol. 15, no. 12, pp. 1271–1273, Dec. 2011.

[18] G. J. Foschini, R. D. Gitlin, and S. B. Weinstein, "On the selection of a two-dimensional signal constellation in the presence of phase jitter and Gaussian noise," *Bell Syst. Techn. J.*, vol. 52, no. 6, pp. 927–965, Jul./Aug. 1973.

[19] S. N. Hulyalkar, "64 QAM signal constellation which is robust in the presence of phase noise and has decoding complexity," U.S. Patent 5 832 041, Nov. 3, 1998.

[20] L. Yang, S. Xu, and H. Yang, "Design of circular signal constellations in the presence of phase noise," in *Proc. 4th Int. Conf. Wireless Commun. Netw. Mobile Comput.*, 2008, pp. 1–8.

[21] T. Pfau, X. Liu, and S. Chandrasekhar, "Optimization of 16-ary quadrature amplitude modulation constellations for phase noise impaired channels," in *Proc. 37th Eur. Conf. Exhibit. Opt. Commun.*, 2011, pp. 1–3.

[22] A. P. T. Lau and J. M. Kahn, "Signal design and detection in presence of nonlinear phase noise," *J. Lightw. Technol.*, vol. 25, no. 10, pp. 3008–3016, Oct. 2007.

[23] L. Beygi, E. Agrell, and M. Karlsson, "Optimization of 16-point ring constellations in the presence of nonlinear phase noise," in *Proc. Opt. Fiber Commun. Conf. Expo. Nat. Fiber Opt. Eng. Conf.*, 2011, pp. 1–3.

[24] C. Hager, A. Graell i Amat, A. Alvarado, and E. Agrell, "Design of APSK constellations for coherent optical channels with nonlinear phase noise," *IEEE Trans. Commun.*, vol. 61, no. 8, pp. 3362–3373, Aug. 2013.

[25] F. Kayhan and G. Montorsi, "Constellation design for channels affected by phase noise," in *Proc. IEEE Int. Conf. Commun. (ICC)*, 2013, pp. 3154–3158.

[26] R. Krishnan, A. Graell i Amat, T. Eriksson, and G. Colavolpe, "Constellation optimization in the presence of strong phase noise," *IEEE Trans. Commun.*, vol. 61, no. 12, pp. 5056–5066, Dec. 2013.

[27] F. Kayhan and G. Montorsi, "Constellation design for memoryless phase noise channels," *IEEE Trans. Wireless Commun.*, vol. 13, no. 5, pp. 2874–2883, May 2014.

[28] B.-J. Kwak, N.-O. Song, B. Park, and D. S. Kwon, "Spiral QAM: A novel modulation scheme robust in the presence of phase noise," in *Proc. IEEE 68th Veh. Technol. Conf.*, 2008, pp. 1–5.

[29] C. Du et al., "Experimental verification of phase noise robust spiral constellation for THz and optical communication," in *Proc. IEEE Asia Pac. Microw. Conf. (APMC)*, 2017, pp. 426–429.

[30] A. Ugolini, A. Piemontese, and T. Eriksson, "Spiral constellations for phase noise channels," *IEEE Trans. Commun.*, vol. 67, no. 11, pp. 7799–7810, Nov. 2019.

[31] M. A. Tariq, H. Mehrpouyan, and T. Svensson, "Performance of circular QAM constellations with time varying phase noise," in *Proc. IEEE 23rd Int. Symp. Pers. Indoor Mobile Radio Commun. (PIMRC)*, 2012, pp. 2365–2370.

[32] B. Zheng, L. Deng, M. Sawahashi, and N. Kamiya, "High-order circular QAM constellation with high LDPC coding rate for phase noise channels," in *Proc. 20th Int. Symp. Wireless Pers. Multimedia Commun. (WPMC)*, 2017, pp. 196–201.

[33] S. Bicaïs and J.-B. Doré, "Design of digital communications for strong phase noise channels," *IEEE Open J. Veh. Technol.*, vol. 1, pp. 227–243, 2020.

[34] P. Wang, N. Ye, J. Li, B. Di, and A. Wang, "Asynchronous multi-user detection for code-domain NOMA: Expectation propagation over 3D factor-graph," *IEEE Trans. Veh. Technol.*, vol. 71, no. 10, pp. 10770–10781, Oct. 2022.

[35] N. Ye, X. Li, H. Yu, L. Zhao, W. Liu, and X. Hou, "DeepNOMA: A unified framework for NOMA using deep multi-task learning," *IEEE Trans. Wireless Commun.*, vol. 19, no. 4, pp. 2208–2225, Apr. 2020.

[36] H. Wang, N. Ye, A. Wang, and B. Di, "Spaceborne cooperative detection for distributed sensing: Overcoming inter-satellite link limitations via deep information bottleneck," *IEEE Trans. Veh. Technol.*, vol. 72, no. 4, pp. 5524–5529, Apr. 2023.

[37] "Digital video broadcasting (DVB); second generation framing structure, channel coding and modulation systems for broadcasting, interactive services, news gathering and other broadband satellite applications; part 1: DVB-S2," ETSI, Sophia Antipolis, France, ETSI EN 302 307–1 V1.4.1, Nov. 2014.

[38] "Digital video broadcasting (DVB); second generation framing structure, channel coding and modulation systems for broadcasting, interactive services, news gathering and other broadband satellite applications; part 2: DVB-S2 extensions (DVB-S2X)," ETSI, Sophia Antipolis, France, ETSI EN 302 307–2 V1.3.1, Jul. 2021.

[39] V. Erceg, "60ghz impairments modeling-ppt," Broadcom Inc., San Diego, CA, USA, IEEE document 11–09-1213–01-00ad, Nov. 2009.

[40] R. Combes and S. Yang, "An approximate ML detector for MIMO channels corrupted by phase noise," *IEEE Trans. Commun.*, vol. 66, no. 3, pp. 1176–1189, Mar. 2018.

[41] T. Minowa, H. Ochiai, and H. Imai, "Phase-noise effects on turbo trellis-coded over M-ary coherent channels," *IEEE Trans. Commun.*, vol. 52, no. 8, pp. 1333–1343, Aug. 2004.

[42] "3rd generation partnership project; technical specification group radio access network; study on supporting NR from 52.6 GHz to 71 GHz (release 17) ," 3GPP, Sophia Antipolis, France, 3GPP Rep. TR 38.808, version 1.0.1, Mar. 2021.

XIAORUI YAN received the B.E. degree from Hunan University, Changsha, China, in 2021. She is currently pursuing the M.Eng. degree with the Beijing Institute of Technology, Beijing, China. Her research interests include wireless communications, 5G evolution and beyond, deep learning, constellation optimization, and waveform.

PEISEN WANG is currently pursuing the Ph.D. degree in communication and information systems with the Beijing Institute of Technology, Beijing, China. His research interests include satellite communications, physical-layer communications, waveform, and nonorthogonal signal processing.

AIHUA WANG (Member, IEEE) received the B.Eng. degree in communication and information systems from Hebei University, Baoding, China, in 1986, the M.Sc. degree in communication and information systems from Xidian University, Xi'an, China, in 1993, and the Ph.D. degree in communication and information systems from the Beijing Institute of Technology, Beijing, China, in 2001, where she is currently a Full Professor with the School of Information Science and Electronics. She has published more than 40 journal and conference papers. She also holds (or co-holds) more than 20 patents. Her main research interests include nonorthogonal multiple access, nonterrestrial network, waveform, and machine learning.

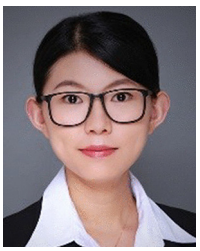

WENJIA LIU received the B.S. degree in electronics engineering and the Ph.D. degree in signal and information processing from Beihang University (formerly, Beijing University of Aeronautics and Astronautics), Beijing, China, in 2011 and 2017, respectively. In 2015, she was a visiting student with the Communications Laboratory, Technische Universität Dresden, Dresden, Germany. She is currently an Advanced Researcher with the Wireless Technology Department, DOCOMO Beijing Laboratories Company Ltd., Beijing, China. Her current research interests include nonorthogonal multiple access, nonorthogonal waveform, full duplex communications, mmWave, and other emerging techniques for 5G evolution and beyond.

XIAOLIN HOU (Senior Member, IEEE) received the B.S. degree in telecommunication engineering and the Ph.D. degree in communication and information system from the Beijing University of Posts and Telecommunications, Beijing, China, in 2000 and 2005, respectively. He is currently the Director of the Wireless Technology Department, DOCOMO Beijing Laboratories Company Ltd., Beijing. He has a strong academic and industrial background and has been actively contributing to 4G and 5G research, standardization, and trials. His current research interests include 5G evolution and beyond, including massive MIMO, mmWave, flexible duplex, NOMA, waveform, URLLC, cellular V2X, and the applications of artificial intelligence in physical-layer design.

JUAN LIU received the B.S. degree in electronics engineering and the M.S. degree in signal and information processing from Beihang University (formerly, Beijing University of Aeronautics and Astronautics), Beijing, China, in 2015 and 2018, respectively. She is currently a Researcher with the Wireless Technology Department, DOCOMO Beijing Laboratories Company Ltd. Her current research interests lie in the area of nonorthogonal waveform and full duplex for 5G evolution and beyond.

NENG YE (Member, IEEE) received the B.S. and Ph.D. degrees from the Beijing Institute of Technology, China, in 2015 and 2021, respectively, where he is currently an Assistant Professor with the School of Cyberspace Science and Technology. His research interests include waveform, nonterrestrial wireless communications, multiuser communications, and intelligent signal processing. He received the Best Ph.D. Thesis Award of China Education Society of Electronics in 2022 and the Young Elite Scientists Sponsorship Program by China Association for Science and Technology in 2022. He has been an Editor of the *Journal of Electronics and Information Technology* since 2021. He was a Lead Guest Editor of *Sensors and Electronics* from 2021 to 2023.